2004

The Energetics of the Hydrogenolysis, Dehydrohalogenation, and Hydrolysis of 4,4‘-Dichloro-diphenyl-trichloroethane from ab Initio Electronic Structure Theory

eric J. Bylaska, *Pacific Northwest National Laboratory*
David A. Dixon, *Pacific Northwest National Laboratory*
Andrew R. Felmy, *Pacific Northwest National Laboratory*
Edoardo Apra, *Pacific Northwest National Laboratory*
Theresa L. Windus, *Pacific Northwest National Laboratory*, et al.

The Energetics of the Hydrogenolysis, Dehydrohalogenation, and Hydrolysis of 4,4′-Dichloro-diphenyl-trichloroethane from ab Initio Electronic Structure Theory

Eric J. Bylaska,* David A. Dixon,† and Andrew R. Felmy

Fundamental Sciences, Pacific Northwest National Laboratory, P.O. Box 999, Richland, Washington 99352

Edoardo Aprà and Theresa L. Windus

William R. Wiley Environmental Molecular Sciences Laboratory, Pacific Northwest National Laboratory, P.O. Box 999, Richland, Washington 99352

Chang-Guo Zhan

Division of Pharmaceutical Sciences, College of Pharmacy, University of Kentucky, 907 Rose Street, Room 501B, Lexington, Kentucky 40536

Paul G. Tratnyek

OGI School of Science & Engineering, Oregon Health & Science University, 20000 NW Walker Road, Beaverton, Oregon 97006-8921

Received: November 10, 2003; In Final Form: April 20, 2004

Electronic structure methods were used to calculate the aqueous reaction energies for hydrogenolysis, dehydrochlorination, and nucleophilic substitution by OH^- of 4,4′-DDT. Thermochemical properties $\Delta H_f°$ (298.15 K), $S°$ (298.15 K, 1 bar), ΔG_S (298.15 K, 1 bar) were calculated by using ab initio electronic structure calculations, isodesmic reactions schemes, gas-phase entropy estimates, and continuum solvation models for a series of DDT type structures $(p-C_6H_4Cl)_2-CH-CCl_3$, $(p-C_6H_4Cl)_2-CH-CCl_2•$, $(p-C_6H_4Cl)_2-CH-CHCl_2$, $(p-C_6H_4Cl)_2-C=CCl_2$, $(p-C_6H_4Cl)_2-CH-CCl_2OH$, $(p-C_6H_4Cl)_2-CH-CCl(=O)$, and $(p-C_6H_4Cl)_2-CH-COOH$. On the basis of these thermochemical estimates, the overall aqueous reaction energetics of hydrogenolysis, dehydrochlorination, and hydrolysis of 4,4′-DDT were estimated. The results of this investigation showed that the dehydrochlorination and hydrolysis reactions have strongly favorable thermodynamics in the standard state, as well as under a wide range of pH conditions. For hydrogenolysis with the reductant aqueous Fe(II), the thermodynamics are strongly dependent on pH, and the stability region of the $(p-C_6H_4Cl)_2-CH-CCl_2•_{(aq)}$ species is a key to controlling the reactivity in hydrogenolysis. These results illustrate the use of ab initio electronic structure methods to identify the potentially important environmental degradation reactions by calculation of the reaction energetics of a potentially large number of organic compounds with aqueous species in natural waters.

I. Introduction

The amount of 4,4′-dichloro-diphenyl-trichloroethane (4,4′-DDT), a potent insecticide, in the environment has been steadily declining since it was banned over thirty years ago[1] because of its catastrophic impact on environment.[2] However, because of its widespread use and its resistance to degradation in the soil, 4,4′-DDT and its metabolites 4,4′-dichloro-diphenyl-dichloroethane (4,4′-DDD) and 4,4′-dichloro-diphenyl-dichloroethene (4,4′-DDE) are still omnipresent in the environment today. Among the chemical reactions that contribute to the environmental degradation of organochlorine compounds such as 4,4′-DDT are hydrogenolysis, dehydrohalogenation, and hydrolysis. Surprisingly, there have been few detailed studies of these reactions for 4,4′-DDT, and many of the basic parameters for these reactions (including thermodynamic heats of reaction, free-energies of solvation, and kinetic rates) are not known.

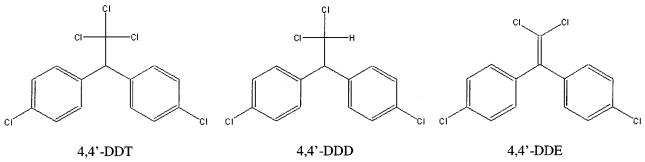

4,4'-DDT 4,4'-DDD 4,4'-DDE

Under anaerobic reducing conditions, hydrogenolysis converts 4,4′-DDT into 4,4′-DDD.[3] This two-electron-transfer reaction most likely occurs in two sequential steps. The first electron transfer results in the dissociation of a chloride anion and the formation of a p,p′-dichloro-diphenyl-dichloroethyl radical

$$(p-C_6H_4Cl)_2-CH-CCl_3 + 1e^- \rightarrow (p-C_6H_4Cl)_2-CH-CCl_2• + Cl^- \quad (1a)$$

The second electron-transfer leads to the protonation of the radical to form 4,4′-DDD.

* Corresponding author. Email: Eric.Bylaska@pnl.gov.
† Current address: Department of Chemistry, University of Alabama, Tuscaloosa, AL 35487-0036.

10.1021/jp0312316 CCC: $27.50
Published on Web 06/10/2004

$$(p-C_6H_4Cl)_2-CH-CCl_2\bullet + 1e^- + H^+ \rightarrow (p-C_6H_4Cl)_2-CH-CHCl_2 \quad (1b)$$

Often in parallel with hydrogenolysis, especially above pH 8, dehydrochlorination may be significant, converting 4,4′-DDT into 4,4′-DDE.

$$(p-C_6H_4Cl)_2-CH-CCl_3 + OH^- \rightarrow (p-C_6H_4Cl)_2-C{=}CCl_2 + H_2O + Cl^- \quad (2)$$

This reaction is generally believed to occur by a bimolecular E2 elimination, in which OH^- abstracts the proton away from the central carbon with concerted loss of chloride from the trichloromethyl carbon.[4]

In addition to reduction and elimination reactions, nucleophilic substitution reactions can lead to dechlorination by substitution with a variety of anions, mainly OH^-, but also SH^-, HCO_3^-, F^-, and so forth. Our previous work on other organochlorine compounds has shown that a wide variety of these dechlorinations by nucleophilic substitutions are thermodynamically favorable.[5] Even if nucleophilic substitution reactions are expected to be slow in terms of kinetics and are not usually considered as degradation pathways for 4,4′-DDT, these reactions may become important on time scales relevant to groundwater systems. In OH^-, the nucleophilic substitution reaction, eq 3a, which results in a p,p′-dichloro-diphenyl-dichloroethanol,

$$(p-C_6H_4Cl)_2-CH-CCl_3 + OH^- \rightarrow (p-C_6H_4Cl)_2-CH-CCl_2OH + Cl^- \quad (3a)$$

$$(p-C_6H_4Cl)_2-CH-CCl_2OH \rightarrow (p-C_6H_4Cl)_2-CH-CCl(=O) + H^+ + Cl^- \quad (3b)$$

$$(p-C_6H_4Cl)_2-CH-CCl(=O) + OH^- \rightarrow (p-C_6H_4Cl)_2-CH-COOH + Cl^- \quad (3c)$$

and the subsequent reactions, (eqs 3b and 3c), which are expected to be fast, combine to produce a p,p′-dichloro-diphenyl-dichloroethanoic acid. Insight into this atypical degradation pathway and its connection to the dehydrochlorination reaction of 4,4′-DDT may be inferred from hydrolysis studies of 1,1,1-trichloroethane (CH_3CCl_3), which is chemically similar to 4,4′-DDT.[6] Several reactivity studies of CH_3CCl_3 have shown that both dehydrochlorination and hydrolysis pathways are possible.[6] In pure water at 10 °C, CH_3CCl_3 hydrolyzes predominately to 1,1-dichloroethene, whereas at 70 °C, it hydrolyzes predominately to acetic acid. By analogy to these experimental results, it seems to reason that at the typical ambient temperatures present in the environment, 4,4′-DDT is likely to hydrolyze predominately to 4,4′-DDE rather than to p,p′-dichloro-diphenyl-dichloroethanoic acid at typical environmental temperatures.

We and others have been using computational chemistry methods to study the environmental degradation of relatively simple organochlorine compounds[5,7−10] and with this study we are extending our work to include more complex molecules such as 4,4′-DDT. Our focus is on obtaining accurate predictions of the enthalpies and free energies of reactions under ambient conditions. To calculate the solution-phase energies of reactions 1−3, we used ab initio electronic structure calculations, isodesmic reactions schemes, gas-phase entropy estimates, and continuum solvation models. Of course, favorable thermodynamics is a necessary, albeit not complete, condition for these reactions to take place. Our objective is not only to elucidate the specific reaction energies but also to develop and test computational approaches that can be used to study a wider variety of organochlorine compounds, as well as reaction kinetics. Future work will focus on detailed reaction mechanisms and barriers for these reactions.

Although ab initio electronic structure methods are constantly being developed and improved, current methods are rarely able to give heats of formations of a broad class for molecules with error limits of less than a few kcal/mol.[11−13] Only when very large basis sets such as the correlation-consistent basis sets,[14] high-level treatments of correlation energy such as coupled cluster methods (CCSD(T)),[15−17] and small correction factors such as core-valence correlation energies and relativistic effects are included will the heat of formation from ab initio electronic structure methods be accurate to within 1 kcal/mol. Although one can now accurately calculate the heats of formation of molecules with up to 6−10 first-row atoms, such high-level calculations are extremely demanding and it is not possible to use these methods to calculate the energetics of compounds as large as 4,4′-DDT given current computational resources. In addition to issues associated with ab initio electronic structure methods, our objective here, the determination of free energies of reaction in solution, also requires solvation and entropic contributions to be included in addition to changes in enthalpy. In this study, separate computational steps are used to calculate electronic energies, entropies, and solvation effects. First, the enthalpies of formation of gas-phase $(p-C_6H_4Cl)_2-CH-CCl_3$, $(p-C_6H_4Cl)_2-CH-CCl_2\bullet$, $(p-C_6H_4Cl)_2-CH-CHCl_2$, $(p-C_6H_4Cl)_2-C{=}CCl_2$, $(p-C_6H_4Cl)_2-CH-CCl_2OH$, $(p-C_6H_4Cl)_2-CH-CCl(=O)$, and $(p-C_6H_4Cl)_2-CH-COOH$ compounds are calculated. Second, the calculated geometries and vibrations are then used to calculate gas-phase entropies. Third, these combined calculations yield the gas-phase free energy of formation for these compounds. Fourth, solvation calculations are used to account for the effect of solvent on the molecular energetics. In such calculations, the basic assumption is that bonding relations within the compounds do not change substantially when going from the gas phase to the solution phase. The reaction energies in both the gas phase and solution phase can then be estimated, because the necessary thermodynamic quantities are known either from experiment or obtained from our calculations.

In section II, the computational methods used in this work are described. Calculations for the enthalpies of formation in the gas-phase of $(p-C_6H_4Cl)_2-CH-CCl_3$, $(p-C_6H_4Cl)_2-CH-CCl_2\bullet$, $(p-C_6H_4Cl)_2-CH-CHCl_2$, $(p-C_6H_4Cl)_2-C{=}CCl_2$, $(p-C_6H_4Cl)_2-CH-CCl_2OH$, $(p-C_6H_4Cl)_2-CH-CCl(=O)$, and $(p-C_6H_4Cl)_2-CH-COOH$ are reported in section III. The difficulties associated with calculating absolute heats of formation from atomization energies are avoided by using isodesmic reactions. The choice of this method is based on results from many studies, which show that using isodesmic reactions leads to excellent agreement with experiment.[18,19] Section IV reports the calculations of the gas-phase entropies using standard statistical mechanical expressions for the vibrational, rotational, and translational entropy contributions. Section V reports the calculations of the solvation energies using the COSMO continuum solvation model.[20] Such a treatment of solvation is more computationally efficient than explicitly doing supermolecule + continuum simulations with explicit water molecules. It has been shown to give solvation energies within a few kcal/mol, which for this study is adequate considering the errors in the gas-phase enthalpies of formation. In section VI, we provide

estimates to aqueous reaction energetics for the dehydrochlorination, nucleophilic substitution, and hydrogenolysis reactions. Concluding remarks are given in section VII.

II. Ab Initio and Continuum Solvation Calculations

All of the ab initio calculations in this study were performed with the NWChem program suite[21] unless noted below. The gas-phase geometries for the neutral and radical compounds were optimized and harmonic frequency vibrational energies were calculated. Tables SM-1 and SM-2 of the Supporting Information contain the electronic energies and thermal vibration energies at 298.15 K for all of the compounds studied. Most of the ab initio calculations in this study were performed at the density functional theory (DFT)[22] and second-order Møller−Plesset perturbation theory (MP2)[23] levels. The Kohn−Sham equations of DFT[24] were solved using the local density approximation (LDA)[25] and the gradient-corrected PBE96,[26] B3LYP,[27,28] and PBE0[29] exchange-correlation functionals. DFT calculations were performed using the DZVP2 basis set.[30] Similarly, MP2 calculations were done with the cc-pVDZ basis set.[14,31−34] The DZVP2 and cc-pVDZ basis sets were obtained from the Extensible Computational Chemistry Environmental Basis Set Database.[35] Certain calculations performed in this study required higher accuracy and were done at the G3(MP2) level[36] with the Gaussian-98 program suite.[37] G3(MP2) calculations are slightly more accurate for compounds than the G2 and G2(MP2) levels[11,12] which preceded it because of the inclusion of core-valence and relativistic effects, and it is comparable in efficiency to the G2(MP2) level. The accuracy of G3(MP2) is quite good and it has reproduced experimental atomization energies to within a few kcal/mol for a large number of organic molecules.[36]

Solvation energies for rigid solutes that do not react strongly with water can be approximated as a sum of noncovalent electrostatic, cavitation, and dispersion energies. The electrostatic contributions to the solvation energies were estimated by using the self-consistent reaction field theory of Klamt and Schüürmann (COSMO),[20] with the cavity defined by the united atom model.[38] The dielectric constant of water used for all of the solvation calculations was 78.4. This continuum model can be used with a variety of ab initio electronic structure calculations in the NWChem program suite including LDA, PBE96, B3LYP, and PBE0. Calculated gas-phase geometries were used to perform these calculations. The irregular solvent cavities for these molecules caused convergence problems, and the solute cavities had to be sufficiently refined for the COSMO calculations to converge. The solvent cavity discretization was generated from the surface of nonoverlapping spheres that were discretized by an iterative refinement of triangles starting from a regular octahedron. Three refinement levels, which is equivalent to 128 points per sphere, were used to define the solvent cavity in these calculations. This refinement parameter was chosen on the basis of a series of COSMO LDA calculations for $(p-C_6H_4Cl)_2-CH-CCl_3$ at increasing refinements. The calculations (Table 1) showed that reasonable convergence (<0.5 kcal/mol) was found when three refinement levels were used.

The cavitation and dispersion contributions to the solvation energy are less straightforward to handle because the interactions take place at short distances. There are several proposed ways to do this.[39−46] One of the simplest approaches for estimating these terms is to use empirically derived expressions that depend only on the solvent accessible surface area. A widely used

TABLE 1: LDA Calculations of the Electrostatic Solvation Energy for $(p-C_6H_4Cl)_2-CH-CCl_3$ at Increasing Levels of Refinement of the COSMO Method

refinement levels	points per atom	cavity surface points	molecular surface area (Å^2)	electrostatic solvation energy (kcal/mol)
1	8	52	409.1	−8.27
2	32	181	363.7	−13.45
3	128	704	354.2	−14.80
4	512	2812	353.8	−15.11

parametrized formula of this type has been given by Sitkoff et al.[44]

$$\Delta G_{cav+disp} = \gamma A + b \tag{4}$$

where γ and b are constants set to 5 cal/mol-Å^2 and 0.86 kcal/mol, respectively. Sitkoff et al. fit the constants γ and b to the experimentally determined free energies of solvation of alkanes[47] by using a least-squares fit. This built on earlier work of the same group as shown in eq 5[42]

$$\Delta G_{cav+disp} = \gamma A \tag{5}$$

where A is the solvent accessible surface area and γ is a constant set to 25 cal/mol-Å^2. The solvent accessible surface area in eq 4 is defined by using a solvent probe with a radius of 1.4 Å rolled over the solute surface defined by van der Waal Radii (i.e., H = 1.2 Å, C = 1.5 Å, O = 1.4 Å, Cl = 1.8 Å). The solvent accessible surface areas were calculated using the VEGA program, Release 1.5.0.92.[48] In this study, we also used the methods contained in the Gaussian 98 program package[37] to yield these terms. The approach here estimates these terms using expressions derived from statistical mechanical models of fluids, where the dispersion and repulsion contributions were calculated using the method of Floris et al.[41] and the cavity formation contribution was calculated using the scaled particle theory of Pierotti.[39]

Chemical equilibrium models were used in this study to calculate aqueous phase species distributions. All calculations of this type were performed using the GMIN chemical equilibrium program developed by A. R. Felmy.[49] The GMIN application package includes chemical models, based on the Pitzer electrolyte equations,[50,51] which calculate liquid−solid-gas equilibria in complex brine systems by globally minimizing the free energy of a system at constant temperature and pressure. The mathematical algorithms used to solve for equilibrium are described in the work of Harvie and Weare.[52] Thermodynamic data for all Fe(II) and Fe(III) species were taken from Martell and Smith.[53]

III. Gas-Phase Enthalpies of Formation

The enthalpies of formation of $(p-C_6H_4Cl)_2-CH-CCl_3$, $(p-C_6H_4Cl)_2-CH-CCl_2\bullet$, $(p-C_6H_4Cl)_2-CH-CHCl_2$, $(p-C_6H_4Cl)_2-C{=}CCl_2$, $(p-C_6H_4Cl)_2-CH-CCl_2OH$, $(p-C_6H_4Cl)_2-CH-CCl(=O)$, and $(p-C_6H_4Cl)_2-CH-COOH$ were calculated by using an isodesmic strategy based on the following reaction:

$$(p-C_6H_4Cl)_2\text{-}R + 2C_6H_6 + CH_4 \rightarrow (C_6H_5)_2-CH_2 + 2C_6H_5Cl + H_2R \tag{6}$$

with $R \equiv {=}CH-CCl_3$, ${=}CH-CCl_2\bullet$, ${=}CH-CHCl_2$, ${=}C{=}CCl_2$, ${=}CH-CCl_2OH$, ${=}CH-CCl(=O)$, and ${=}CH-COOH$. For each compound, the reaction enthalpy of eq 5 was calculated from the electronic, thermal, and vibrational energy differences at

TABLE A1: Experimental and High Quality ab Initio Gas-Phase Enthalpies of Formation (kcal/mol) Used in Computations

compd	ΔH_f°	compd	ΔH_f°	compd	ΔH_f°
CH_3	34.821[b]	CCl_3-CCl_3	−32.079[b]	C_6H_6	19.82[b]
CCl_3	19.000[b]	$CH_2Cl-CHCl_2$	−35.400[b]	C_6H_5Cl	13.01[b]
CH_2Cl_2	−22.100[c]	CCl_3-CH_3	−34.51[b]	$CH_3-C_6H_5$	11.95[b]
CH_3Cl	−19.320[c]	$CHCl_2-CH_3$	−30.5[b]	$CH_3-(C_6H_4Cl)$	4.57[c]
CH_4	−17.880[c]	CH_2Cl-CH_3	−26.83[b]	$CH_2-(C_6H_5)_2$	39.39[b]
CH_3-CCl_2OH	−75.51[a]	CH_3-CH_3	−20.04[b]		
CH_3-CClO	−60.07[b]				
CH_3-CCl_2	12.3[a]				
$H_2C=CCl_2$	0.53[b]				

[a] Values obtained from isodesmic calculations at the G3(MP2) level, see text. [b] Experimental ref 55. [c] Experimental ref 69.

TABLE 2: Gas-Phase Enthalpies of Formation ΔH_f^o (298.15 K) (kcal/mol) from Isodesmic Reactions[a]

compd	LDA/DZVP2	PBE96/DZVP2	B3LYP/DZVP2	PBE0/DZVP2	MP2/cc-pVDZ
$(p-C_6H_4Cl)_2-CH-CCl_3$	10.37	15.39	17.32	16.91	5.66
$(p-C_6H_4Cl)_2-CH-CHCl_2$	12.79	16.52	17.74	17.90	7.60
$(p-C_6H_4Cl)_2-CH-CCl_2$	54.95	58.34	59.85	60.02	
$(p-C_6H_4Cl)_2-C=CCl_2$	35.38	38.88	40.55	40.85	32.88
$(p-C_6H_4Cl)_2-CH-CCl_2OH$	−32.06	−26.12	−24.14	−24.60	−36.24
$(p-C_6H_4Cl)_2-CH-CCl(=O)$	−16.33	−13.74	−13.08	−12.12	−19.97
$(p-C_6H_4Cl)_2-CH-COOH$	−60.41	−58.04	−57.32	−56.33	−63.56

[a] Experimental and ab initio total energy values used to determine these enthalpies of formations are given in Table A1 and as Supporting Information. All quantities are in kcal/mol. See eq 3.1 and 3.2 for definitions of isodesmic reactions.

298.15 K at a consistent level of theory. UMP2 calculations were not performed for $(p-C_6H_4Cl)_2-CH-CCl_2\bullet$ because the UHF reference state contained a significant amount of spin-contamination ($S^2 = 1.14$ as compared to an ideal value of $S^2 = 0.75$). Given these reaction energies, the enthalpy of formation of the unknown $(p-C_6H_4Cl)_2$-*R* compounds can then be calculated by using Hess's law with the calculated enthalpy change and the known heats of formation of the other five compounds, which were obtained from experiment or high-quality ab initio estimates, for example,

$$\Delta H_f\,(p-C_6H_4Cl)_2\text{-}R = \Delta H_f\,(C_6H_5)_2-CH_2(\text{exp}) + 2\,\Delta H_f\,C_6H_5Cl(\text{exp}) + \Delta H_f\,CH_2R(\text{exp}) - 2\,\Delta H_f\,C_6H_6(\text{exp}) - \Delta H_f\,CH_4(\text{exp}) - \Delta H_r(\text{calc}) \quad (7)$$

The errors associated with these calculations are expected to be small, because eq 5 has an equal number of like bonds on the left-hand and right-hand sides of the reaction. In addition, the errors associated with the dispersion interaction between the two bridged phenyl groups are expected to largely cancel, since both sides of eq 5 contain two bridged phenyl groups.

Table A1 contains high-quality ab initio estimates for the enthalpies of formation of $CH_3-CCl_2\bullet$ and CH_3-CCl_2OH because experimental values were not available. The enthalpies of formation of these two compounds were estimated by calculating the following isodesmic reactions energies

$$CH_3-CCl_2\bullet + CH_3-CH_3 \rightarrow CH_3-CHCl_2 + CH_3-CH_2\bullet \quad (8)$$

$$CH_3-CCl_2OH + CH_3-CH_3 \rightarrow CH_3-CHCl_2 + CH_3-CH_2OH \quad (9)$$

at the G3(MP2) level, together with the experimental enthalpies of formation of CH_3-CH_3, CH_3-CHCl_2, $CH_3-CH_2\bullet$, and CH_3-CH_2OH. For comparison purposes, we calculated the enthalpies of formation of CH_3-CCl_3 and CH_3-CClO using a similar strategy based on the following isodesmic reactions

$$CH_3-CCl_3 + CH_3-CH_3 \rightarrow CH_3-CHCl_2 + CH_3-CH_2Cl \quad (10)$$

$$CH_3-CClO + CH_3-CH_3 \rightarrow CH_3-CHCl_2 + CH_3-CHO \quad (11)$$

The G3(MP2) isodesmic values for $\Delta H_f^o(CH_3-CCl_3)$ and $\Delta H^o_f(CH_3-CClO)$ are −34.1 kcal/mol and −59.3 kcal/mol as compared to the experimental values of -34.51 ± 0.38 kcal/mol[54,55] and -60.07 ± 0.12 kcal/mol.[55,56]

The gas-phase enthalpies of formation for the $(p-C_6H_4Cl)_2$-*R* compounds calculated by using the theoretical isodesmic reaction, eq 5, are reported in Table 2. The various ab initio energies needed for the isodesmic calculations and isodesmic reaction energies calculated are given as Supporting Information. Several of the $(p-C_6H_4Cl)_2$-*R* compounds can have a variety of isomeric forms. Specifically, for $(p-C_6H_4Cl)_2-CH-CHCl_2$, $(p-C_6H_4Cl)_2-CH-CCl_2OH$, $(p-C_6H_4Cl)_2-CH-CCl(=O)$, and $(p-C_6H_4Cl)_2-CH-COOH$, different isomers are yielded upon rotation of the R1 fragment of $(p-C_6H_4Cl)_2-CH-R1$. Relative ab initio energies for several low-lying isomers found in our calculations are given in the Supporting Information. One strategy would be to use only the lowest energy isomers. The errors associated with this approximation are not expected to be significant, since the low-lying isomers were calculated to be within 1 kcal/mol of the lowest lying isomer or were inaccessible to interconversion (see section IV). However, rather than using only the lowest energy isomers, we chose instead to estimate a canonical vibrational partition function, *Q*, for each compound, including in it the rotational energy levels associated with rotating R1 fragment and the chlorophenyl fragments (see Section IV). The enthalpy correction (Supporting Information) is then calculated by using the following formula.[57]

$$\delta H = RT^2\frac{d(\ln Q)}{dT} + RT \quad (12)$$

Experimental and high level ab initio calculations of enthalpies of formation needed to apply the various isodesmic strategies are given in Table A1. Table 2 contains the values based on the isodesmic reactions at the LDA/DZVP2, PBE96/

TABLE 3: Isodesmic Reaction Energies (kcal/mol) to Benchmark the Computational Methods

isodesmic reactions	exp	LDA/DZVP2	PBE96/DZVP2	B3LYP/DZVP2	PBE0/DZVP2	MP2/cc-pVDZ
$C_6H_6+C_2H_6 \rightarrow CH_3C_6H_5+CH_4$	−5.71	−7.02	−5.50	−5.59	−5.11	−6.01
$2(CH_3C_6H_5) \rightarrow (H_2C(C_6H_5)_2+CH_4$	−2.39	−2.97	−1.37	0.18	−2.47	−4.99
$CH_3C_6H_5+C_6H_6+C_2H_6 \rightarrow H_2C(C_6H_5)_2 + 2CH_4$	−8.10	−9.99	−6.87	−5.40	−7.58	−10.99
$CH_3Cl+C_6H_6 \rightarrow CH_4+C_6H_5Cl$	−5.37	−7.52	−5.65	−4.21	−4.84	−7.66
$C_2Cl_6+C_2H_6 \rightarrow 2CH_3CCl_3$	−16.90	−16.31	−18.62	−20.73	−19.37	−12.86
$CH_3CHCl_2+CH_3CH_2C\,l \rightarrow CH_3CCl_3+C_2H_6$	2.78	4.29	5.85	7.57	7.12	2.54
$2CH_3CH_2Cl \rightarrow CH_3CHCl_2+C_2H_6$	3.12	0.91	1.85	2.91	2.64	0.40
$CH_2ClCHCl_2 \rightarrow CH_3CCl_3$	0.89	0.01	1.21	2.53	2.25	0.17
$CH_3CCl_3+CH_4 \rightarrow CH_3CHCl_2+CH_3Cl$	2.57	1.26	−1.33	−3.35	−2.84	2.44
$CH_3CCl_3+CH_4 \rightarrow CH_3CH_2Cl+CH_2Cl_2$	3.46	4.09	0.60	−1.62	−0.90	5.76
average error		1.31	1.59	2.80	2.01	1.82
maximum error		2.21	3.90	5.92	5.41	4.04

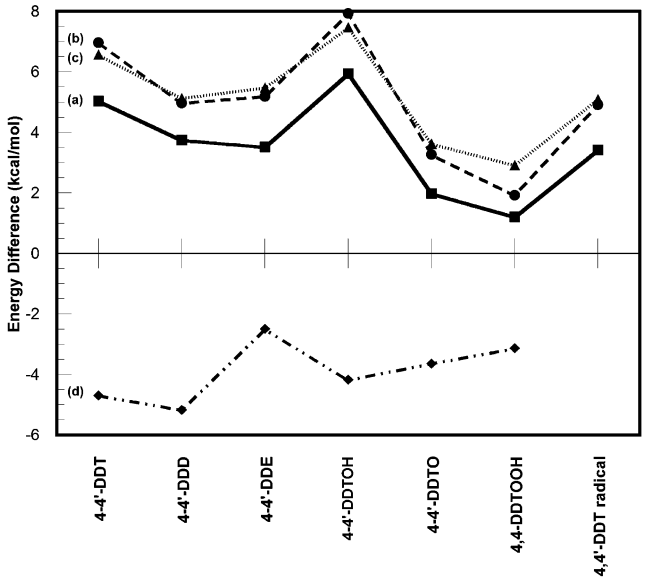

Figure 1. Enthalpy differences (kcal/mol) of (a) PBE96/DZVP2, (b) B3LYP/DZVP2, (c) PBE0/DZVP2, and (d) MP2/cc-pVDZ calculations relative to SVWN5/DZVP2 calculations.

DZVP2, B3LYP/DZVP2, PBE0/DZVP2, and MP2/cc-pVDZ levels. As expected, the calculated heats of formation between the gradient-corrected DFT methods are similar with differences at most about a few kcal/mol. Differences between LDA and gradient-corrected DFT levels are larger, up to 8 kcal/mol for $(p-C_6H_4Cl)_2-CH-CCl_2OH$, with the LDA values always being more negative. Even more significant differences are between gradient-corrected DFT and MP2 levels. Differences of up to 12 kcal/mol are seen between the gradient-corrected DFT and MP2 levels, and as found at the LDA level, the MP2 values are more negative than the gradient-corrected values. In addition, the MP2 values are more negative than the LDA values by 3−5 kcal/mol. Although the differences are larger than expected, the differences appear to be systematic. Figure 1 contains a plot of energy differences relative to the LDA/DZVP2 level calculations. As this plot demonstrates, the relative energy differences are reasonably consistent even though large differences are seen between the gradient-corrected DFT and MP2 levels. Several factors might be contributing to the additional stabilization seen at the MP2 level, including dispersion, basis set superposition, and differences between the dipole−dipole energies of the bridged chlorophenyl groups, although we would be surprised if any of these factors are likely to be worth 10 kcal/mol.

Even though the origin of the differences is unresolved, it is interesting to compare the accuracy of the different ab initio levels for isodesmic reactions that contain molecules used in our isodesmic strategy, that is, eq 5. To determine which values should be used, we benchmarked the results by evaluating isodesmic reaction energies for several similar reactions as shown in Table 3. Table 3 contains the heats of reaction for a set of isodesmic reactions that contain molecules used in our isodesmic strategy, that is, eq 5. For these 10 isodesmic reactions, the LDA/DZVP2 level performed the best overall, and the B3LYP/DZVP2 level performed the worst overall. The average (maximum) errors from experiment were 1.31 (2.21) kcal/mol, 1.59 (3.90) kcal/mol, 2.90 (5.92) kcal/mol, 2.01 (5.41) kcal/mol, and 1.82 (4.04) kcal/mol for the LDA/DZVP2, PBE96/DZVP2, B3LYP/DZVP2, PBE0/DZVP2, and MP2/cc-pVDZ methods, respectively. At the LDA level, the reaction energies are mostly more negative than experiment. For MP2, most of the energies are also too negative and in most cases the errors in terms of the sign match the LDA signs. The largest error for MP2 is for the reaction $C_2Cl_6+C_2H_6 \rightarrow 2CH_3CCl_3$, where MP2 is too positive. The gradient-corrected DFT methods all predict reaction energies that are significantly too negative. On the basis of these results, we have chosen to use the LDA values.

IV. Gas-Phase Entropies

The gas-phase standard virtual entropies of the $(p-C_6H_4-Cl)_2$-*R* compounds were calculated by using formulas derived from statistical mechanics.[57,58] Results based on accurate structures and frequencies can often provide more accurate values than those determined by direct thermal measurements.[58−60] However, the situation is complicated for the $(p-C_6H_4Cl)_2$-*R* compounds as these molecules contain internal degrees of freedom (torsions) that may not be well described by normal vibrations. Significant coupling between the torsional and other vibrational degrees of freedom may be present. For example, $(p-C_6H_4Cl)_2-CH-CCl_3$ contains three loosely rotating fragments (i.e., R1, R2, and R3), where R1 is the rotating trichloromethyl fragment, and R2 and R3 are the dangling chlorphenyl fragments which may also rotate. Estimating accurate entropies in this situation can be a computationally very demanding task, requiring a detailed knowledge of the coupled torsional potentials of the molecule, which could involve sampling many configurations. Therefore, entropy estimates for the compounds in this study are not expected to be as accurate as for those entropy estimates of smaller organochlorine compounds such as CCl_4, which do not have low-energy torsions. However, given the difficulty associated with calculating the partition function with full anharmonicity, these should be reasonably reliable.[61]

There are two limiting cases for the motion of molecules that contain rotating tops. The first limiting case is that where the barrier impeding the rotation of a fragment is very high; the second is that the rotation is essentially unhindered. For highly hindered rotations, the fragment will not rotate except at

extremely high temperatures. In this case, the rotation can be considered as a torsional oscillation at ambient temperatures and thus can be treated as a regular vibration in its contribution to the entropy. For nearly free rotation (the second limiting case), one must treat the contribution to the entropy in a different way and add an entropy contribution due to each internal bond rotation, for example, by using the expressions proposed by Pitzer and Gwinn.[58,62] Unfortunately, for $(p-C_6H_4Cl)_2$-*R* compounds, neither one of these limits may be entirely satisfactory.

In the current study, we explicitly solved for the energy levels of the rotational Schrödinger equation of each rotor (R1, R2, and R3) and then used this as input into a canonical partition function of the bond rotation to estimate its entropy. The rotational Schrödinger equation for a rotor is written as[63]

$$\frac{-\hbar^2}{2I_r}\frac{\partial^2\psi}{\partial^2\varphi} + V(\varphi)\psi = \epsilon\psi \tag{13}$$

where I_r is the reduced moment of inertia, and $V(\varphi)$ is the rotational potential. For molecules containing a single top attached to a rigid frame, the reduced moment of inertia is[58,62]

$$I_r = I_{top}\left[1 - I_{top}\left(\frac{\lambda_{top-A}}{I_A} + \frac{\lambda_{top-B}}{I_B} + \frac{\lambda_{top-C}}{I_C}\right)\right] \tag{14}$$

with I_{top} the moment of inertia of the top itself, λ_{top-A} the cosine of the angle between the axis of the top and the axis of the principle moment of inertia I_A of the whole molecule, and λ_{top-B} and λ_{top-C} the projections of the top axis onto the axes of the other principle moments of inertia I_B and I_C. The potential energy surfaces for torsions were calculated by rotating each fragment while keeping the other rotating fragments fixed at the optimized geometry. Each rotational potential energy surface, $V(\varphi)$, was mapped out using LDA/DZVP2 energy calculations in $d\theta = 5°$ rotating increments (72 points). The energy levels of the rotational Schrödinger equation were solved by fast Fourier transforming the extended rotational potential energy surface

$$\tilde{V}(k) = \frac{1}{N}\sum_{i=0}^{N-1} V(i)\exp\left(i\frac{2\pi jk}{N}\right) \tag{15}$$

and then diagonalizing the following Hamiltonian matrix using $N = 1152$ points (high-frequency modes of the rotational potential energy surface were set to zero by linearly interpolating $V(\varphi)$ to use $N = 1152$ points)

$$H(i,j) = \begin{cases} \frac{1}{2I_r}i^2\delta_{i,j} + \tilde{V}(\mathrm{mod}[i-j,N]), \text{ for } 0 \le i \le \frac{N}{2}, 0 \le j \le \frac{N}{2} \\ \tilde{V}(\mathrm{mod}[i-j+N,N]), \text{ for } 0 \le i \le \frac{N}{2}, \frac{N}{2} < j < N \\ \tilde{V}(\mathrm{mod}[i-N-j,N]), \text{ for } \frac{N}{2} < i < N, 0 \le j \le \frac{N}{2} \\ \frac{1}{2I_r}(i-N)^2\delta_{i,j} + \tilde{V}(\mathrm{mod}[i-j,N]) \text{ for } \frac{N}{2} < i < N, \frac{N}{2} < j < N \end{cases} \tag{16}$$

to obtain rotational energy levels, ϵ_i. A large number of rotational levels were needed to ensure that the calculation of the canonical partition function was converged.

The entropy of the rotor is then calculated by using the following formulas.[58]

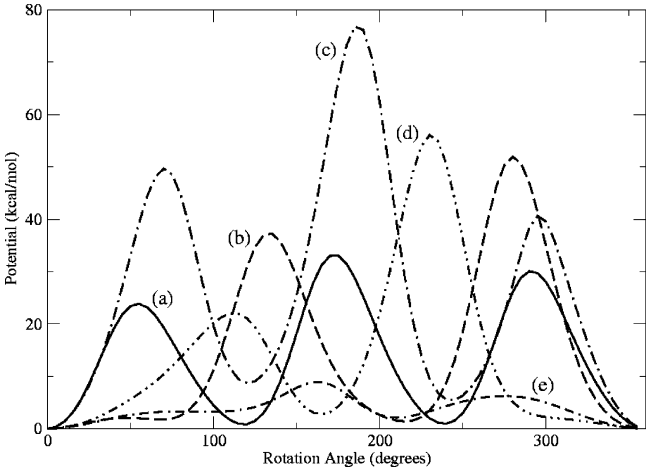

Figure 2. Rotation potential energy surface of the R1 fragment ($(p-C_6H_4Cl)_2-CH-$R1) for (a) $(p-C_6H_4Cl)_2-CH-CCl_3$, (b)$(p-C_6H_4Cl)_2-CH-CCl_2\bullet$, (c) $(p-C_6H_4Cl)_2-CH-CCl_2OH$, (d) $(p-C_6H_4Cl)_2-CH-CCl(=O)$, and (e) $(p-C_6H_4Cl)_2-CH-COOH$.

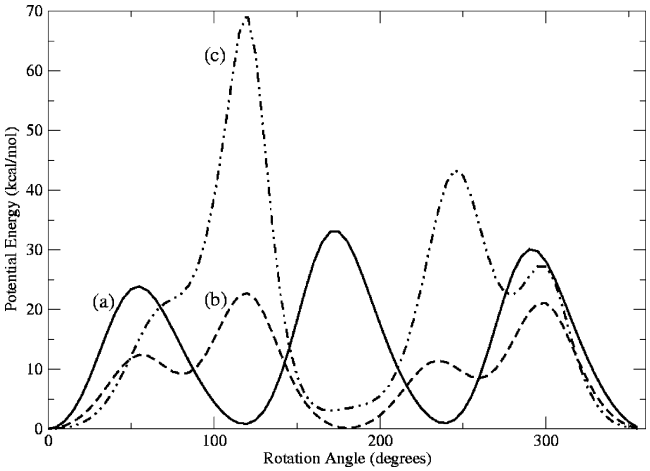

Figure 3. Torsional potential energy surface of the (a) R1 $=CCl_3$ fragment, (b) first R2$=(C_6H_4Cl)$ fragment, and (c) second R3$=(C_6H_4Cl)$ fragment for $(p-C_6H_4Cl)_2-CH-CCl_3$.

$$S_{rotor}{}^{o} = R\ln Q_{rotor} + RT\frac{d(\ln Q_{rotor})}{dT} \tag{17}$$

$$Q_{rotor} = \frac{\sum_{i=0}^{N-1}\exp\left(-\frac{\epsilon_i}{RT}\right)}{\sigma} \tag{18}$$

where σ is the number of indistinguishable positions of the rotor (e.g., $\sigma = 3$ for the R1 $= CCl_3$ rotor). Potential energy plots for these hindered rotations are shown in Figures 2 and 3. The barriers for interconversion of the R2 and R3 fragments are quite large for all of the compounds; however, the potential surfaces are very flat near the minima resulting in harmonic frequencies of 50 cm^{-1} or less. In contrast, the rotation barriers of the R1 fragments are large for some of the compounds ($(p-C_6H_4Cl)_2-CH-CCl_3$, $(p-C_6H_4Cl)_2-CH-CHCl_2$, $(p-C_6H_4Cl)_2-C=CCl_2$, $(p-C_6H_4Cl)_2-CH-CCl_2OH$) and low for the others ($(p-C_6H_4Cl)_2-CH-CCl_2\bullet$, $(p-C_6H_4Cl)_2-CH-CCl(=O)$, and $(p-C_6H_4Cl)_2-CH-COOH$). Clearly, a higher dimensional rotational energy surface that contains a combination of all three rotating fragments will have probably have lower barriers than those found with each top interacting statically with the other two tops without relaxing their torsional modes. The separable approximation that we have made thus represents higher bounds

TABLE 4: Translational, Rotational, Vibrational, and Electronic[b] Entropy Contributions $S_{trans+rot+vib}°$ (298.15 K, 1bar) to the Total Entropy (cal/mol-K)[a]

compd	LDA/DZVP2	PBE96/DZVP2	B3LYP/DZVP2	PBE0/DZVP2
$(p-C_6H_4Cl)_2-CH-CCl_3$	126.59	127.30	124.89	124.13
$(p-C_6H_4Cl)_2-CH-CHCl_2$	122.45	124.13	122.69	122.13
$(p-C_6H_4Cl)_2-CH-CCl_2•$	120.85	120.62	119.17	118.44
$(p-C_6H_4Cl)_2-C=CCl_2$	124.44	124.37	123.12	122.64
$(p-C_6H_4Cl)_2-CH-CCl_2OH$	125.49	126.85	125.52	124.81
$(p-C_6H_4Cl)_2-CH-CCl(=O)$	119.85	120.85	118.94	118.56
$(p-C_6H_4Cl)_2-CH-COOH$	117.92	119.54	117.34	117.24

[a] Atomic standard states: $S°(1/2\ H_2) = 15.617$, $S°$(C-graphite) $= 1.372$, $S°(1/2\ O_2) = 24.515$, $S°(1/2\ Cl_2) = 27.845$; ref 69. [b] The entropy of $(p-C_6H_4Cl)_2-CH-CCl_2•$ includes an electronic entropy of $R \ln 2 = 1.38$ cal/mol-K.

TABLE 5: Hindered Rotation Entropy Estimates (cal/mol-K)

compd	$S_{hindered}°$	$S_{free}°$	$\Delta S_{free-hindered}°$
$(p-C_6H_4Cl)_2-CH-CCl_3$	11.45	23.34	11.89
$(p-C_6H_4Cl)_2-CH-CHCl_2$	12.03	23.56	11.53
$(p-C_6H_4Cl)_2-CH-CCl_2$	14.34	23.50	9.16
$(p-C_6H_4Cl)_2-C=CCl_2$	8.44	15.31	6.87
$(p-C_6H_4Cl)_2-CH-CCl_2OH$	10.96	25.24	14.28
$(p-C_6H_4Cl)_2-CH-CCl(=O)$	15.51	24.28	8.77
$(p-C_6H_4Cl)_2-CH-COOH$	15.83	23.58	7.77

to the rotational barriers and hence a lower bound to the entropy of the rotating fragments. Conversely, setting $V(\varphi)$ to zero defines an upper bound to the entropy of the rotating fragment.

The total virtual entropy $S°$ at 298.15 K of the $(p-C_6H_4Cl)_2$-*R* compounds considered in this study consists of translational, rotational, vibrational, electronic, and hindered rotational components. Notwithstanding the fact that the hindered rotations may be described by harmonic frequencies for some of the compounds, we chose not to use them because their potential surface is very flat ($\omega < 50\ cm^{-1}$). The translational, rotational, vibrational, and electronic components of the total virtual entropy are provided in Table 4. Very little difference is seen between the different DFT methods in the calculated values of $S°_{trans+rot+vib}$, with differences of at most a few cal/mol-K. The average absolute differences from LDA/DZVP2 vibrational calculations are 0.95, 0.92, and 1.4 cal/mol-K for the PBE96/DZVP2, B3LYP/DZVP2, and PBE0/DZVP2 vibrational calculations, repectively. Two different estimates to the hindered rotational components of the total virtual entropy are provided in Table 5. For these estimates, LDA/DZVP2 optimized geometries were used. The lower bound estimate, $S°_{hindered}$, is taken as the sum of the entropies of the three rotors, using the potential energy surfaces from LDA/DZVP2 energy calculations. Similarly, the higher bound estimate, $S°_{free}$, is taken as the sum of the entropies of the three rotors, whose potential energy surfaces were set to zero. Fairly large differences are seen between the lower and higher bound estimates, and given the strongly interacting character of the three rotors, it is difficult to say with absolute certainty which estimate is better. However, it is anticipated that the lower bound estimate will be a more reasonable estimate of the entropy.

The values of ΔH_f and $S°$ in Tables 2, 4, and 5 can be used to calculate the gas-phase standard Gibbs free energy of formation at 298.15 K of the $(p-C_6H_4Cl)_2$-*R* compounds. This is done by calculating the entropy of formation, $\Delta S_f°$, which is obtained by subtracting off the entropies of the atomic standard states, from the virtual entropy of the species. For example, $\Delta S_f°((p-C_6H_4Cl)_2-CH-CCl_3)$ and $\Delta G_f°((p-C_6H_4Cl)_2-CH-CCl_3)$ are calculated from the following expressions:

$$\Delta S_f°\ ((p-C_6H_4Cl)_2-CH-CCl_3) = S°((p-C_6H_4Cl)_2-CH-CCl_3) - (14S°(\text{C-graphite}) + 5S°(1/2Cl_2) + 9S°(1/2H_2)) \quad (19)$$

$$\Delta G_f°((p-C_6H_4Cl)_2-CH-CCl_3) = \Delta H_f°((p-C_6H_4Cl)_2-CH-CCl_3) - T\Delta S_f°((p-C_6H_4Cl)_2-CH-CCl_3) \quad (20)$$

For example, by using the LDA/DZVP2 values for $S°((p-C_6H_4Cl)_2-CH-CCl_3)$ and $\Delta H_f°((p-C_6H_4Cl)_2-CH-CCl_3)$ (isodesmic), the entropy of formation is $\Delta S_f°((p-C_6H_4Cl)_2-CH-CCl_3) = -158.394$ cal/mol-K and the Gibbs free energy of formation is $\Delta G_f°\ ((p-C_6H_4Cl)_2-CH-CCl_3) = 57.2$ kcal/mol. A table of calculated $\Delta G_f°$ values at 298.15 K is given in the Supporting Information.

V. Free Energies of Solvation

The solvation thermodynamics of $(p-C_6H_4Cl)_2-CH-CCl_3$, $(p-C_6H_4Cl)_2-CH-CCl_2•$, $(p-C_6H_4Cl)_2-CH-CHCl_2$, $(p-C_6H_4Cl)_2-C=CCl_2$, $(p-C_6H_4Cl)_2-CH-CCl_2OH$, $(p-C_6H_4Cl)_2-CH-CCl(=O)$, and $(p-C_6H_4Cl)_2-CH-COOH$ were estimated by using the procedure outlined above. The noncovalent electrostatic contributions to the solvation energy at various electronic structure levels using the COSMO model are given in Table 6. These calculations were performed by using the optimized gas-phase geometries at the specific computational level. Differences between the various electronic structure levels are negligible in these calculations. The average absolute differences from COSMO LDA/DZVP2 calculations are 0.51, 0.79, and 0.59 kcal/mol, respectively, for the COSMO PBE96/DZVP2, COSMO B3LYP/DZVP2, and COSMO PBE0/DZVP2. Calculated solvent accessible surface areas, based on gas-phase geometries from LDA/DZVP2 calculations, and three different

TABLE 6: Electrostatic Solvation Energies ΔG_S (electrostatic) (kcal/mol)

compd	COSMO/LDA/DZVP2	COSMO/PBE96/DZVP2	COSMO/B3LYP/DZVP2	COSMO/PBE0/DZVP2
$(p-C_6H_4Cl)_2-CH-CCl_3$	−14.80	−14.30	−13.86	−14.26
$(p-C_6H_4Cl)_2-CH-CHCl_2$	−20.56	−19.85	−19.41	−19.79
$(p-C_6H_4Cl)_2-CH-CCl_2$	−16.45	−15.81	−15.39	−15.73
$(p-C_6H_4Cl)_2-C=CCl_2$	−6.40	−6.29	−6.35	−6.49
$(p-C_6H_4Cl)_2-CH-CCl_2OH$	−19.11	−19.47	−19.47	−19.52
$(p-C_6H_4Cl)_2-CH-CCl(=O)$	−16.42	−15.49	−15.79	−15.72
$(p-C_6H_4Cl)_2-CH-COOH$	−22.66	−22.31	−21.33	−21.73

TABLE 7: Solvent Accessible Surface Areas (SAS) and Non-Electrostatic Solvation Energies

compd	SAS (Å^2)	ΔG_S (cav+disp) (kcal/mol)			ΔG_S (entropy loss) (kcal/mol)
		Sitkoff[44]	Honig[42]	G98	
$(p-C_6H_4Cl)_2-CH-CCl_3$	501.5	3.37	12.54	8.98	3.41
$(p-C_6H_4Cl)_2-CH-CHCl_2$	490.3	3.31	12.26	7.92	3.59
$(p-C_6H_4Cl)_2-CH-CCl_2$	490.6	3.31	12.27	8.62	4.28
$(p-C_6H_4Cl)_2-C=CCl_2$	486.3	3.29	12.16	7.84	2.52
$(p-C_6H_4Cl)_2-CH-CCl_2OH$	493.0	3.33	12.33	8.18	3.27
$(p-C_6H_4Cl)_2-CH-CCl(=O)$	478.5	3.25	11.96	7.86	4.62
$(p-C_6H_4Cl)_2-CH-COOH$	469.7	3.21	11.74	6.42	4.72

TABLE 8: Total Solvation Energies ΔG_S(total) (kcal/mol)[a]

compd	COSMO/LDA/DZVP2	COSMO/PBE96/DZVP2	COSMO/B3LYP/DZVP2	COSMO/PBE0/DZVP2
$(p-C_6H_4Cl)_2-CH-CCl_3$	−6.12	−5.62	−5.18	−5.58
$(p-C_6H_4Cl)_2-CH-CHCl_2$	−11.76	−11.05	−10.61	−10.99
$(p-C_6H_4Cl)_2-CH-CCl_2$	−6.96	−6.32	−5.90	−6.24
$(p-C_6H_4Cl)_2-C=CCl_2$	1.31	1.42	1.36	1.22
$(p-C_6H_4Cl)_2-CH-CCl_2OH$	−10.61	−10.97	−10.97	−11.02
$(p-C_6H_4Cl)_2-CH-CCl(=O)$	−6.65	−5.72	−6.02	−5.95
$(p-C_6H_4Cl)_2-CH-COOH$	−12.83	−12.48	−11.50	−11.90

[a] For the SCRF theory calculations to conform to the standard state of 1 bar of pressure at 298.15 K in the gas phase, a constant value of 1.90 kcal/mol was added to the SCRF free energies of solvation.

TABLE 9: Heats of Reaction (kcal/mol) for Hydgrogenolysis, Dehydrohalogenation, and Hydrolysis Processes in the Aqueous Phase

	LDA/DZVP2	PBE96/DZVP2	B3LYP/DZVP2	PBE0/DZVP2
		Hydrogenolysis Reactions		
(1a)	−59.07	−60.28	−61.01	−60.38
(1b)	−106.09	−106.25	−106.52	−106.63
(1a+1b)	−165.16	−166.53	−167.53	−167.00
		Dehydrochlorination Reactions		
(2)	−29.43	−31.11	−32.22	−31.33
		Hydrolysis Reactions		
(3a)	−36.56	−36.70	−37.41	−37.12
(3b)	−43.40	−45.35	−46.80	−45.36
(3c)	−39.90	−40.88	−39.45	−39.98
(3a+3b+3c)	−119.86	−122.93	−123.66	−122.46

approximations to the cavity and dispersion contributions are given in Table 7. Differences between the three different cavity dispersion models are as large as 9 kcal/mol. These differences are quite sizable and neither of these models may be entirely satisfactory. However, for our purposes here which is to determine reaction energies, these errors are expected to largely cancel since the compounds are structurally very similar. The solvent accessible surface areas are within 30 Å^2 (out of ∼500 Å^2) of each other, and the corresponding ΔG_s(cav+disp) are within 0.2, 0.8, and 2.6 kcal/mol of each other in the Sitkoff,[44] Honig,[42] and G98 models, respectively.

Table 7 also contains a correction associated with changes in internal rotation that will occur upon solvation. This correction assumes that the solvent completely constrains all three hindered rotations in these compounds. In our previous studies, on smaller and less complicated organochlorine compounds such as CCl_4, we were able to safely neglect the effect that changes in internal vibration and rotation might have on solvation. However, for the compounds in this study the corrections to the solvation energy, associated with changes in internal rotation about the three rotors, may be quite sizable. In a worst case scenario, the solvent will completely constrain the three rotors and reduce the molecular entropy. As shown in Table 7, this could lead to solvation energies being destabilized by 3−5 kcal/mol. In addition, all the compounds in this study contain two very low frequency bending modes ($<100 cm^{-1}$) that may also be constrained by solvation. One is a breathing mode between the two chlorophenyl groups and the other is a side-by-side motion of the two phenyls. Constraining these modes could lead to the solvation energies being stabilized by an additional 1−4 kcal/mol. Table 8 lists the overall free energies of solvation for all the compounds in this study which is obtained by adding the Sitkoff[44] ΔG_S (cav+disp) + ΔG_S (entropy loss) (Table 7) to the ΔG_S (electrostatic) term (Table 6) plus an additional value of 1.90 kcal/mol. The value of 1.90 kcal/mol was added to the overall free energy of solvation, because the standard state in the gas phase in the COSMO model is 1 mol/L at 298.15 K rather than at 1 bar of pressure at 298.15 K. The −5.4 kcal/mol estimate provided for $(p-C_6H_4Cl)_2-CH-CCl_3$ is a few kcal/mol less than the values of Henry's Law constants determined from experiment,[64,65] which places the solvation energy between −1.7 kcal/mol and −2.8 kcal/mol. However, considering the approximations and errors associated with estimating the solvation energies together with the fact that $(p-C_6H_4Cl)_2-CH-CCl_3$ contains very low frequency bending modes that may also be constrained by solvation, the agreement is quite good.

VI. Aqueous-Phase Gibbs Free Energies of Reaction

Table 9 shows the aqueous-phase Gibbs free energies of reaction for the hydrogenolysis (eq 1a and 1b), dehydrochlorination (eq 2), and hydrolysis (eq 3a and 3c) reactions involving DDT and its metabolites. The reaction energies in Table 9 were generated by using the experimental values for $\Delta G_f°(H^+_{(aq)})$, $\Delta G_f°$ $(OH^-_{(aq)})$, $\Delta G_f°$ $(Cl^-_{(aq)})$, $\Delta G_f°$ $(H_2O_{(l)})$, and $\Delta G_f°$ $(e\text{-}_{(aq)})$ given in Table A2, the values for $\Delta G_f°$ $((p-C_6H_4Cl)_2-R_{(g)})$ obtained by using eqs 10−11 with values taken from Tables 2, 4, and 5, and finally the solvation energies, ΔG_s $((p-C_6H_4-$

TABLE A2: Experimental Aqueous-Phase Free Energies of Formation (kcal/mol) Used in Computations

compd	ΔG_f° (298.15 K,aq)
e^-	64.0[a,b]
H^+	0.00
Cl^-	−31.36[c]
OH^-	−37.58[c]
H_2O	−56.675[c]

[a] ΔG_s(e-) = −34.6 kcal/mol from refs 70, 71. [b] E_H° = 98.6 kcal/mol calculated from ΔG_s (H^+) = −263.98 kcal/mol[72] and ΔG_f° (H^+(g)) = 362.58 kcal/mol.[69] [c] ΔG_f°(aq) obtained from experimental ref 69.

$Cl)_2-R_{(g)}$), obtained from Table 8. In agreement with the systematic differences seen in Figure 1, very little difference was seen between the different DFT levels in the reactions energies. The largest standard deviation in reaction energies was 1.93 kcal/mol for the overall hydrolysis reaction, eq (3a+3b+3c). The largest absolute difference was 4.98 kcal/mol between the SVWN5/DZVP2 and B3LYP/DZVP2 reaction energies of overall hydrolysis reaction, eq (3a+3b+3c).

Our results clearly show that the dehydrochlorination and hydrolysis reactions have strongly favorable thermodynamics in the standard state, as well as under a wide range of pH conditions. At first glance, it might be expected that these reactions will not take place at low pH, since OH^- is on the left-hand side of these reactions. However, the standard state free energies are so strongly negative that dehydrochlorination (eq 2) and hydrolysis (eq 3a and 3b) reactions are still favorable in solutions with pH well below 3. Therefore, the outcome of these reactions will always be thermodynamically favorable in natural waters under a wide range of pH conditions. On the other hand, the hydrogenolysis reactions are expected to be strongly affected by the environmental conditions in which they occur. As written, the hydrogenolysis reactions represented by eq 1a and 1b are thermodynamically favorable because the solvated electron is an extremely powerful reductant. This result is of little direct relevance because there are very few environmental sources of solvated electrons, except for remediation technologies involving electron beams,[66] photolysis,[67] or alkali metals.[68]

A reductant that has more direct environmental significance is aqueous Fe(II). During a redox reaction involving organic pollutants, aqueous Fe(II) is oxidized to various forms of Fe(III), including $Fe(OH)_2^+{}_{(aq)}$, $Fe(OH)_4^-{}_{(aq)}$, as well as to a variety of stable solids from $Fe(OH)_{3(am)}$ to goethite. The half-reactions corresponding to these oxidations of Fe(II) (e.g., $Fe^{2+}{}_{(aq)} + H_2O_{(l)} \rightarrow 1e^- + FeOH^{2+}{}_{(aq)} + H^+{}_{(aq)}$) can be combined with the half-reactions represented by eq 1a and 1b to evaluate the thermodynamics of 4,4′-DDT hydrogenolysis by aqueous Fe(II) over a range of pHs. We have performed these chemical equilibrium simulations for cases where the Fe(III) products are $Fe(OH)_2^+{}_{(aq)}$, $Fe(OH)_4^-{}_{(aq)}$, and goethite.

The first chemical equilibrium simulations considered the aqueous phase oxidation of Fe(II) species by 4,4′-DDT to form 4,4′-DDD. Just as with the dehyrochlorination and hydrolysis reactions, we found that hydrogenolysis reactions (eq 1a and 1b) coupled with the oxidation of Fe(II) to $Fe(OH)_2^+{}_{(aq)}$, $Fe(OH)_4^-{}_{(aq)}$, and goethite are thermodynamically favorable across the entire pH range. The formation of 4,4′-DDD was strongly favored by the equilibrium constants for the redox reactions. For example, at pH = 3 the dominant species in solution are $Fe^{2+}{}_{(aq)}$ and $Fe(OH)_2^+{}_{(aq)}$, and the resulting redox reaction is

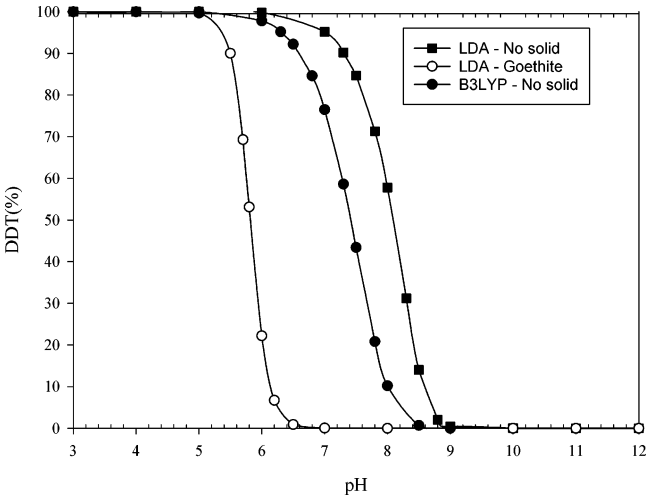

Figure 4. Calculated reduction of 4,4′-DDT for various Fe(II) oxidation reactions.

$$2Fe^{2+}{}_{(aq)} + 4,4'\text{-}DDT_{(aq)} + 2H_2O \rightarrow 4,4'\text{-}DDD_{(aq)} + 2FeOH^{2+}{}_{(aq)} + H^+{}_{(aq)} + Cl^-{}_{(aq)} \quad (21)$$

with an equilibrium constant of log K = 12.1. Thermodynamically, therefore, aqueous Fe(II) is capable of reducing 4,4′-DDT across the entire pH range even when no Fe(III) solid is formed.

Thermodynamics has more impact with respect to the solution phase stability of the intermediate species $(p-C_6H_4Cl)_2-CH-CCl_2\bullet_{(aq)}$. The results of chemical equilibrium calculations show some notable effects of pH. Under acidic conditions, the equilibrium constant for the reduction of 4,4′-DDT to form $(p-C_6H_4Cl)_2-CH-CCl_2\bullet_{(aq)}$ is unfavorable, log K = −15.2 for the reaction,

$$Fe^{2+}{}_{(aq)} + (p-C_6H_4Cl)_2-CH-CCl_{3(aq)} \rightarrow (p-C_6H_4Cl)_2-CH-CCl_2\bullet_{(aq)} + Fe^{3+}{}_{(aq)} + Cl^-{}_{(aq)} \quad (22)$$

but is favorable under strongly basic conditions (i.e., log K = +9.2) for the following reaction.

$$Fe(OH)_4^{2-}{}_{(aq)} + (p-C_6H_4Cl)_2-CH-CCl_{3(aq)} \rightarrow (p-C_6H_4Cl)_2-CH-CCl_2\bullet_{(aq)} + Fe(OH)_4^-{}_{(aq)} + Cl^-{}_{(aq)} \quad (23)$$

In Figure 4 we show the results of chemical equilibrium calculations of redox reactions involving aqueous Fe(II) (arbitrary initial concentration 0.001 M $FeCl_2$) and its ability to form $Fe(OH)_2^+{}_{(aq)}$, $Fe(OH)_4^-{}_{(aq)}$, and goethite in reactions with 4,4′-DDT. From these results, the stability region for the $(p-C_6H_4Cl)_2-CH-CCl_2\bullet_{(aq)}$ species is a key variable in the hydrogenolysis reaction. 4,4′-DDT is stable over $(p-C_6H_4Cl)_2-CH-CCl_2\bullet_{(aq)}$ until the solution pH reaches 6 to 7 for solution phase reactions (no solid precipitation allowed) and pH = 5 to 6 if the precipitation of the more stable goethite is allowed. At higher pH values, $(p-C_6H_4Cl)_2-CH-CCl_2\bullet_{(aq)}$ is stable and DDT should be reduced by Fe(II) species if present in the chemical system. Because of the uncertainty in our thermodynamic estimates, these pH profiles are approximated and must be treated with a degree of skepticism, and errors on the order of 3 pH units are likely. For example, a difference of ∼0.7 pH unit is seen between the LDA and B3LYP estimates which have overall reaction differences of 1.9 kcal/mol.

VII. Summary

Ab initio electronic structure theory, canonical ensemble entropy formulas, and self-consistent reaction field theory were

used to estimate the thermochemical properties, $\Delta H_f°$ (298.15 K), $S°$(298.15 K,1 bar), and ΔG_S(298.15 K, 1bar), of 4,4′-DDT and its metabolites: $(p-C_6H_4Cl)_2-CH-CCl_3$, $(p-C_6H_4Cl)_2-CH-CCl_2•$, $(p-C_6H_4Cl)_2-CH-CHCl_2$, $(p-C_6H_4Cl)_2-C=CCl_2$, $(p-C_6H_4Cl)_2-CH-CCl_2OH$, $(p-C_6H_4Cl)_2-CH-CCl(=O)$, and $(p-C_6H_4Cl)_2-CH-COO$. The most difficult computational step in our thermodynamic estimations was determining the gas-phase enthalpies of formation, $\Delta H_f°$ (298.15 K). For this, a strategy based on isodesmic reactions was used to reduce the error associated with determining $\Delta H_f°$ (298.15 K). This strategy was reliable, especially for predicting overall reaction energies. Even though differences of up to 12 kcal/mol were seen in the values of $\Delta H_f°$ (298.15 K) predicted from different ab initio methods, the relative energy differences and overall reaction energies were consistent within a few kcal/mol. To determine which $\Delta H_f°$ (298.15 K) values were the most reliable, we compared the accuracy of the different ab initio levels for several similar isodesmic reactions that contain molecules used in our isodesmic strategy. These limited tests showed that LDA/DZVP2 calculations performed the best overall, and surprisingly the gradient-corrected DFT methods performed the worst overall.

The calculated thermochemical properties allowed us to estimate the equilibrium product distributions as a function of pH for the hydrogenolysis, dehydrohalogenation, and hydrolysis of 4,4′-DDT. Our chemical equilibrium calculations showed that the dehydrochlorination and hydrolysis reactions have strongly favorable thermodynamics in the standard state, as well as under a wide range of pH conditions. In contrast with these results, chemical equilibrium calculations for the first reductive dehalogenation step in which the reductant was aqueous Fe(II) showed that the formation of the intermediate $(p-C_6H_4Cl)_2-CH-CCl_2•_{(aq)}$ species was strongly dependent on pH. Our results showed that 4,4′-DDT is stable over $(p-C_6H_4Cl)_2-CH-CCl_2•_{(aq)}$ near pH = 6 and below if no solid precipitation is allowed and near pH = 5 and below if goethite precipitates. Furthermore, our results showed that at higher pH values, $(p-C_6H_4Cl)_2-CH-CCl_2•_{(aq)}$ is more stable than 4,4′-DDT.

The results of this study demonstrate that ab initio electronic structure methods in combination with chemical equilibrium methods can be used to calculate the reaction energetics and equilibrium constants of a potentially large number of reactions involving organic compounds in solution, including large and complex molecules such as 4,4′-DDT for which experimental data are unavailable, and can be used to help identify the potentially important environmental degradation reactions. Finally, it is important to emphasize that the thermodynamic quantities presented here are studies to determine if a reaction is even allowed or not. Equally important in understanding these reactions are the height and shape of kinetic barriers existing between the reactants and products including the role of solvent on the reaction pathways. We are currently extending our studies to investigate the role of kinetics for these reactions.

Acknowledgment. A significant portion of this research was supported by the Department of Energy Office of Science Environmental Management Sciences Program (EMSP) (P.G. Tratnyek, PI). Additional support also came from EMSL operations supported by the DOE's Office of Biological and Environmental Research. Some of the calculations were performed at the Molecular Science Computing Facility in the Environmental Molecular Sciences Laboratory at the Pacific Northwest National Laboratory. We also wish to thank the Scientific Computing Staff, Office of Energy Research, U.S. Department of Energy for a grant of computer time at the National Energy Research Scientific Computing Center (Berkeley, CA).

Supporting Information Available: Tables of ab initio total energies and enthalpy corrections for the gas-phase compounds determined from LDA/DZVP2, PBE96/DZVP2, B3LYP/DZVP2, PBE0/DZVP2, and MP2/cc-pVDZ total energy and vibrational calculations. Also, tables containing the total enthalpies from G3(MP2) ab initio calculations, gas-phase Gibbs free energies of formation ΔG_f^o (298.15 K, gas), aqueous-phase Gibbs free energies of formation ΔG_f^o (298.15 K, aq), and relative energies at the LDA/DZVP2 level for low-energy stereoisomers found by rotating the R1 fragment are given. In addition to the Supporting Information available, the optimized structures for all the molecules calculated can be obtained by correspondence with E. J. Bylaska (Eric.Bylaska@pnl.gov). This material is available free of charge via the Internet at http://pubs.acs.org.

References and Notes

(1) Eisenreich, S. J.; Willford, W. A.; Strachan, W. M. J. The Role of atompspheric deposition in organic contaminant cycling in the Great Lakes. In *Intermediate Pollutant Transport: Modelling and Field Measurements*; Allen, D., Ed.; Plenum: New York, 1989.

(2) Carson, R. *Silent Spring*; Houghton Mifflin Co: New York, 2002.

(3) Macalady, D. L.; Tratnyek, P. G.; Grundl, T. J. *J. Contam. Hydrol.* **1986**, *1*, 1.

(4) Wolfe, N. L.; Zepp, R. G.; Paris, D. F.; Baughman, G. L.; Hollis, R. C. *Environ. Sci. Technol.* **1977**, *11*, 1077.

(5) Bylaska, E. J.; Dixon, D. A.; Felmy, A. R. *J. Phys. Chem. A* **2000**, *104*, 610.

(6) Schwarzenbach, R. P.; Gschwend, P. M.; Imboden, D. M. *Environmental Organic Chemistry*; John Wiley & Sons: New York, 1993.

(7) Bylaska, E. J.; Dixon, D. A.; Felmy, A. R.; Tratnyek, P. G. *J. Phys. Chem. A* **2002**, *106*, 11581.

(8) Arnold, W. A.; Wignet, P.; Cramer, C. J. *Environ. Sci. Technol.* **2002**, *36*, 3536.

(9) Nonnenberg, C.; van der Donk, W. A.; Zipzse, H. *Phys. Rev. A* **2002**, *106*, 8708.

(10) Patterson, E. V.; Cramer, C. J.; Truhlar, D. G. *J. Am. Chem. Soc.* **2001**, *123*, 2025.

(11) Curtiss, L. A.; Raghavachari, K.; Redfern, P. C.; Pople, J. A. *J. Chem. Phys.* **1997**, *106*, 1063.

(12) Curtiss, L. A.; Raghavachari, K.; Trucks, G. W.; Pople, J. A. *J. Chem. Phys.* **1991**, *94*, 7221.

(13) Pople, J. A.; Head-Gordon, M.; Fox, D. J.; Raghavachari, K.; Curtiss, L. A. *J. Chem. Phys.* **1989**, *90*, 5622.

(14) Dunning, T. H., Jr. *J. Chem. Phys.* **1989**, *90*, 1007.

(15) Bartlett, R. J. *J. Phys. Chem.* **1989**, *93*, 1697.

(16) Bartlett, R. J.; Stanton, J. F. In *Reviews of Computational Chemistry*; Lipkowitz, K. B., Boyd, D. B., Ed.; VCH Publishers: New York, 1995; Chapter 2.

(17) Kucharski, S. A.; R. J. Bartlett. *J. Adv. Quantum Chem.* **1986**, *18*, 281.

(18) Hehre, W. J.; Radom, L.; Schleyer, P. v. R.; Pople, J. A. *Ab Initio Molecular Orbital Theory*; John Wiley & Sons: New York, 1986.

(19) Dixon, D. A. *J. Phys. Chem.* **1988**, *92*, 86.

(20) Klamt, A.; Schuurmann, G. *J. Chem. Soc., Perkin Trans. 2* **1993**, *1993*, 799.

(21) Straatsma, T. P.; Apra, E.; Windus, T. L.; Dupuis, M.; Bylaska, E. J.; de Jong, W.; Hirata, S.; Smith, D. M. A.; Hackler, M. T.; Pollack, L.; Harrison, R. J.; Nieplocha, J.; Tipparaju, V.; Krishnan, M.; Brown, E.; Cisneros, G.; Fann, G. I.; Fruchtl, H.; Garza, J.; Hirao, K.; Kendall, R.; Nichols, J. A.; Tsemekhman, K.; Valiev, M.; Wolinski, K.; Anchell, J.; Bernholdt, D.; Borowski, P.; Clark, T.; Clerc, D.; Dachsel, H.; Deegan, M.; Dyall, K.; Elwood, D.; Glendening, E.; Gutowski, M.; Hess, A.; Jaffe, J.; Johnson, B.; Ju, J.; Kobayashi, R.; Kutteh, R.; Lin, Z.; Littlefield, R.; Long, X.; Meng, B.; Nakajima, T.; Niu, S.; Rosing, M.; Sandrone, G.; Stave, M.; Taylor, H.; Thomas, G.; van Lenthe, J.; Wong, A.; Zhang, Z. *NWChem, A Computational Chemistry Package for Parallel Computers*, 4.5 ed.; Pacific Northwest National Laboratory: Richland, WA, 2003.

(22) Hohenberg, P.; Kohn, W. *Phys. Rev. B* **1964**, *136*, 864.

(23) Moller, C.; Plesset, M. S. *Phys. Rev.* **1934**, *46*, 618.

(24) Kohn, W.; Sham, L. J. *Phys. Rev.* **1965**, *A140*, 1133.

(25) Vosko, S. H.; Wilk, L.; Nusair, M. *Can. J. Phys.* **1980**, *58*, 1200.

(26) Perdew, J. P.; Burke, K.; Ernzerhof, M. *Phys. Rev. Lett.* **1996**, *77*, 3865.
(27) Becke, A. D. *J. Chem. Phys.* **1993**, *98*, 5648.
(28) Lee, C.; Yang, W.; Parr, R. G. *Phys. Rev. B* **1988**, *37*, 785.
(29) Adamo, C.; Barone, V. *J. Chem. Phys.* **1997**, *110*, 6158.
(30) Godbout, N.; Salahub, D. R.; Andzelm, J.; Wimmer, E. *Can. J. Chem.* **1992**, *70*, 560.
(31) Peterson, K. A.; Kendall, R. A.; Dunning, T. H., Jr. *J. Chem. Phys.* **1993**, *99*, 1930.
(32) Peterson, K. A.; Kendall, R. A.; Dunning, T. H., Jr. *J. Chem. Phys.* **1993**, *99*, 9790.
(33) Woon, D. E.; Dunning, T. H., Jr. *J. Chem. Phys.* **1993**, *98*, 1358.
(34) Woon, D. E.; Dunning, T. H., Jr. *J. Chem. Phys.* **1995**, *103*, 4572.
(35) Feller, D.; Schuchardt, K. Basis sets were obtained from the Extensible Computational Chemistry Environment Basis Set Database, Version 9/12/01, as developed and distributed by the Molecular Science Computing Facility, Environmental and Molecular Sciences Laboratory which is part of the Pacific Northwest Laboratory, P.O. Box 999, Richland, WA 99352, and funded by the U.S. Department of Energy, 2001.
(36) Curtiss, L. A.; Raghavachari, K.; Redfern, P. C.; Rassolov, V.; Pople, J. A. *J. Chem. Phys.* **1998**, *109*, 7764.
(37) Frisch, M. J.; Trucks, G. W.; Schlegel, H. B.; Scuseria, G. E.; Robb, M. A.; Cheeseman, J. R.; Zakrzewski, V. G.; Montgomery, J. A., Jr.; Stratmann, R. E.; Burant, J. C.; Dapprich, S.; Millam, J. M.; Daniels, A. D.; Kudin, K. N.; Strain, M. C.; Farkas, O.; Tomasi, J.; Barone, V.; Cossi, M.; Cammi, R.; Mennucci, B.; Pomelli, C.; Adamo, C.; Clifford, S.; Ochterski, J.; Petersson, G. A.; Ayala, P. Y.; Cui, Q.; Morokuma, K.; Malick, D. K.; Rabuck, A. D.; Raghavachari, K.; Foresman, J. B.; Cioslowski, J.; Ortiz, J. V.; Stefanov, B. B.; Liu, G.; Liashenko, A.; Piskorz, P.; Komaromi, I.; Gomperts, R.; Martin, R. L.; Fox, D. J.; Keith, T.; Al-Laham, M. A.; Peng, C. Y.; Nanayakkara, A.; Gonzalez, C.; Challacombe, M.; Gill, P. M. W.; Johnson, B. G.; Chen, W.; Wong, M. W.; Andres, J. L.; Head-Gordon, M.; Replogle, E. S.; Pople, J. A. *Gaussian 98*, revision A.4; Gaussian, Inc.: Pittsburgh, PA, 1998.
(38) Barone, V.; Cossi, M.; Tomasi, J. *J. Chem. Phys.* **1997**, *107*, 3210.
(39) Pierotti, R. A. *J. Phys. Chem.* **1965**, *69*, 281.
(40) Huron, M. J.; P. Claverie. *J. Phys. Chem.* **1974**, *78*, 1853.
(41) Floris, F. M.; Tomasi, J.; Pascual Ahuir, J. L. *J. Comput. Chem.* **1991**, *12*, 784.
(42) Honig, B.; Sharp, K. A.; Yang, A. *J. Phys. Chem.* **1993**, *97*, 1101.
(43) Tomasi, J.; Persico, M. *Chem. Rev.* **1994**, *94*, 2027.
(44) Sitkoff, D.; Sharp, K. A.; Honig, B. *J. Phys. Chem.* **1994**, *98*, 1978.
(45) Cramer, C. J.; Truhlar, D. G. *Chem. Rev.* **1999**, *99*, 2161.
(46) Eckert, F.; Klamt, A. *AIChE J.* **2002**, *48*, 369.
(47) Ben-Naim, A.; Marcus, Y. J. *J. Chem. Phys.* **1984**, *81*, 2016.
(48) Pedretti, A.; Vistoli, G. *VEGA*, standard ed., Release 1.5.092; Win9x/ME/NT/2000/XP ed., 2003.
(49) Felmy, A. R. Chapter 18. In *Soil Science Society of Americal Special Publication;* **1995**, *42*, 377.
(50) Pitzer, K. S. *Acc. Chem. Res.* **1977**, *10*, 371.
(51) Pitzer, K. S. Theory: Ion interaction approach. In *Activity coefficients in electrolyte solutions*; Pytckowicz, R. M., Ed.; CRC Press: Boca Raton, FL, 1979; p 157.
(52) Harvie, C. E.; Greenberg, J. P.; Weare, J. H. *Geochim. Cosmochim. Acta* **1987**, *51*, 1045.
(53) Martell, A. E.; Smith, R. M. *Crically Selected Stability Constants of Metals Complexes Database*, Version 2.0; NIST Standard Reference Data Program: Gaithersburg, MD, 1995.
(54) Hu, A. T.; Sinke, G. C.; Mintz, M. J. *J. Chem. Thermodyn.* **1972**, *4*, 239.
(55) Chase, J., M. W. *Phys. Chem. Ref. Data, Monograph No. 9* **1998**, *9*, 1.
(56) Devore, J. A.; O'Neal, H. E. *J. Phys. Chem.* **1969**, *73*, 2644.
(57) McQuarrie, D. A. *Statistical Mechanics*, 1st ed.; Harper & Row: New York, 1973.
(58) Herzberg, G. *Molecular Spectra and Molecular Structure II. Infared and Raman Spectra of Polyatomic Molecules*, 2nd ed.; D. Van Nostrand Company, Inc: New York, 1947.
(59) Urey, H. G. *J. Am. Chem. Soc.* **1923**, *45*, 1445.
(60) Tolman, R. C.; Badger, R. M. *J. Am. Chem. Soc.* **1923**, *45*, 2277.
(61) East, A. L. L.; Radom, L. *J. Chem. Phys.* **1997**, *106*, 6655.
(62) Pitzer, K. S.; Gwinn, W. D. *J. Chem. Phys.* **1942**, *10*, 428. Pitzer, K. S. *Quantum Chemistry*; Prentice-Hall: New York, 1953.
(63) McQuarrie, D. A. *Quantum Chemistry*; University Science Books: Sausalito, CA, 1983.
(64) Mackay, D.; Shiu, W. Y. *J. Phys. Chem. Ref. Data* **1981**, *10*, 1175.
(65) Brimblecombe, P. *Air Composition & Chemistry*; Cambridge University Press: Cambridge, 1986.
(66) Mak, F. T.; Zele, S. R.; Cooper, W. J.; Kurucz, C. N.; Waite, T. D.; Nickelsen, M. G. *Water Res.* **1987**, *31*, 219.
(67) Zepp, R. G.; Braun, A. M.; Hoigne, J.; Leenheer, J. A. *Environ. Sci. Technol.* **1987**, *21*, 485.
(68) Getman, G. D.; Pittman, C. U., Jr. Solvated Electron Reductions: A Versatile Alternative for Waste Remediation. In *Chemical Degradation Methods for Wastes and Pollutants: Environmental and Industrial Applications*; Tarr, M. A., Ed.; Marcel Dekker: New York, 2003.
(69) Wagman, D. D. *J. Phys. Chem. Ref. Data* **1982**, *11*, Suppl. 2.
(70) Shiraishi, H.; Sunaryo, G. R.; Ishigure, K. *J. Phys. Chem.* **1994**, *98*, 5164.
(71) Coe, J. V. *Int. Rev. Phys. Chem.* **2001**, *20*, 33.
(72) Tissandier, M. D.; Cowen, K. A.; Feng, W. Y.; Gundlach, E.; Cohen, M. H.; Earhart, A. D.; Coe, J. V.; Tuttle, T. R., Jr. *J. Phys. Chem. A* **1998**, *102*, 7787.
(73) Appendix: Experimental and high quality ab initio values.